Estimation of the Upper Tropospheric Relative Humidity Field from METEOSAT Water Vapor Image Data

JOHANNES SCHMETZ AND OLLI M. TURPEINEN*

European Space Operations Centre, Darmstadt, METEOSAT Exploitation Project, Federal Republic of Germany

(Manuscript received 24 August 1987, in final form 19 January 1988)

ABSTRACT

A retrieval method is described for estimating a mean column value of the upper tropospheric relative humidity (UTH) from radiance measurements in the 6.3 μm channel of the geostationary satellite METEOSAT. The physical retrieval method is based on an efficient radiative transfer scheme which uses the temperature forecast profiles from the European Centre for Medium Range Weather Forecasts (ECMWF) as ancillary data. Theoretical radiances for the given temperature profile and a set of fixed upper tropospheric humidities are employed to relate the observed radiance to a mean humidity for a layer between 600 and 300 hPa. The retrieval is confined to areas with neither medium- nor high-level clouds.

A calibration procedure of the 6.3 μm channel is described which uses the radiative transfer scheme with measured radiosonde profiles of temperature and humidity and collocated satellite measurements. An example of the UTH product and a comparison with radiosondes is presented. An estimate of the error of the UTH is obtained from a sensitivity test of the radiation scheme to errors in the input profiles. Both the sensitivity test and the comparison with radiosondes yield absolute error estimates for the UTH of 10%–15%.

1. Introduction

There is an increasing interest in the analysis of humidity data for the initialization of numerical forecast models. Obviously a global analysis of humidity fields is only possible with the horizontal coverage provided by satellite data. Raschke and Bandeen (1967) employed the two spectral channels at 8–13 μm and at 5.7–6.9 μm on board the TIROS-IV spacecraft to infer the relative humidity of the upper troposphere over large portions of the earth. While Hayden et al. (1981) state that the retrieval of detailed vertical humidity structures is difficult from the sounder data of the present polar orbiting satellites, they also demonstrate that mean values for columns of a few hundred millibars can be derived with confidence.

Recently Illari (1987) has shown that the use of three layer column values of the moisture derived from TIROS-N data have a beneficial impact on the humidity analyses and the forecasts of the ECMWF. She also pointed out that the humidity analysis is especially important in the tropics where the relaxation time of the vertical motions is of the order of 3 days as compared to about 12 h in midlatitudes. An accurate moisture analysis is therefore a prerequisite for a reduction of the spin-up time of the hydrological cycle of the forecast model, especially in the tropical region.

Limited information i.e., single column values for the upper tropospheric humidity (hereafter UTH) can be derived from the imaging radiometer channel at 6.3 μm onboard the geostationary satellite METEOSAT. The possibility of using satellite measurements within the 6.3 μm band of water vapor to estimate a mean relative humidity of the upper troposphere at levels above about 600 hPa has been shown by Möller as early as 1961. Poc et al. (1980) have shown that there exists a relation between the radiance field in the water vapor channel and the water vapor mass between about 600 and 300 hPa pressure level.

The purpose of the present work is to describe the operational algorithm which is used at the European Space Operations Centre (ESOC) to estimate the UTH, a mean value of the relative humidity for the column from 600 to 300 hPa. The content of the paper is as follows: section 2 comprises general aspects of the satellite and the data; section 3 describes the physical retrieval method employing a radiative transfer scheme; section 4 examines the performance of the radiation scheme by comparison with other models; section 5 outlines the calibration procedure and section 6 follows with an error analysis. A final section provides a summary and conclusions.

2. The satellite and data preprocessing

The geostationary METEOSAT satellite observes the earth with an imaging radiometer in three channels:

* Present affiliation: Recherche en Prevision Numerique, 2121 Transcanadienne, Dorval, PQ. Canada H9P 1J3.

Corresponding author address: Dr. Johannes Schmetz, European Space Operations Centre, MEP, Robert Bosch Str. 5, 6100 Darmstadt West Germany.

- the solar spectrum (VIS) between 0.4 and 1.1 μm,
- the infrared window region (IR) between 10.5 and 12.5 μm, and
- the water vapor (WV) absorption band between 5.7 and 7.1 μm.

Images are taken at half-hourly intervals with spatial resolution at the subsatellite point of 2.5 × 2.5 km for the VIS, and 5 × 5 km for the IR and the WV channels.

The radiometric data are digitized with 8 bits for the IR channel and 6 bits for the WV and VIS channels. A one-countstep corresponds to a change in brightness temperature of about 0.5°C at 280 K in the IR channel and to about 0.9°C at 260 K in the WV channel. The noise equivalent $\Delta T(NE\Delta T)$ is about half of those values; i.e., for the WV channel at a scene temperature of 260 K, ΔT is about 0.5°C.

From the METEOSAT image data the following meteorological products are derived operationally: cloud motion vectors, cloud analysis, cloud top height, sea surface temperature, precipitation index, and the UTH. An overview of the operational aspects involved in the derivation of the various products has been given by de Waard et al. (1984).

Common to all meteorological products is the segment processing. The METEOSAT image is subdivided into segments of 32 × 32 IR pixels, corresponding to about 160 × 160 km at the subsatellite point and about 200 × 200 km as a mean value. The aim of the segment processing is to objectively classify the dominating scenes within a segment via a histogram analysis. Because of the increasing distortion of the images towards the horizon, the routine processing is confined to 55° of the great circle arc of the subsatellite point. The size of a segment has been chosen under the constraints of providing a reasonable sample for the histogram analysis while still resolving features compatible with the grid size of a global forecast model. The meteorological products are derived daily at fixed times specific to each product. At present, the UTH is derived at 0000 and 1200 UTC. It is disseminated as SATOB code via the Global Telecommunications System (GTS). The total processing area contains more than 3500 segments and, on average, the UTH is derived for about 2000 segments identified as containing neither medium- nor high-level cloud. A typical example is shown in Fig. 7a. All products are edited and manually quality controlled before dissemination.

3. Methodology

Assuming a plane-parallel atmosphere and neglecting scattering of the longwave infrared radiation, the spectral radiance measured by a radiometer onboard a satellite can be expressed by (e.g., Liou 1980)

$$L(\theta) = \phi L_s(\theta)\tau(\theta, p_s) + \int_{p_s}^{0} \phi B[T(p)] \frac{\partial \tau(\theta, p)}{\partial p} d_p \quad (1)$$

where L_s is the effective radiance exiting the surface, θ the zenith angle of the satellite, p the pressure, p_s the surface pressure, τ the spectral transmittance between $p = 0$ and the pressure level indicated, $T(p)$ the temperature profile, B the spectral Planck function, and ϕ describes the spectral response of the satellite radiometer. A subscript denoting a spectral dependence of the various quantities has been omitted.

Equation (1) states that the radiance received at the satellite is a function of the surface exitance, the transmission properties of the atmosphere and the vertical temperature structure. In our approach we assume an adequate knowledge of the temperature structure, available as forecast data from the ECMWF, and seek a solution for the transmittance (humidity) variations. Our retrieval method is based on a look-up table derived from radiative transfer calculations for a set of fixed UTH. The table interrelates the WV and IR radiances or counts to the UTH. In the text, the table is referred to as "UTH Table."

a. Radiation scheme

The near real-time estimation of the humidity fields requires an efficient radiative transfer model. An analytical solution to the radiative transfer equation has been chosen. The scheme and its application to the METEOSAT IR channel has been described by Schmetz 1986. Here a summary is provided of the most important features:

- In differential form the radiative transfer equation for a non-scattering medium reads

$$\mu dL/d\delta = B(T) - L \quad (2)$$

with μ being the cosine of the zenith angle and δ the optical depth, which increases along the direction of the radiance. Equation (2) is known as Schwarzschild's equation (Liou 1980).

- Allowing the black-body source function $B(T)$ to vary linearly over optical depth, Eq. (2) is solved by

$$L = C \exp(-\delta/\mu) + B_0 + (\delta - \mu)\Delta B/\delta_t \quad (3)$$

where B_0 is the Planck function at the bottom of a model layer, ΔB the difference between B_0 and the Planck function at the top of the layer, and δ_t the total optical depth of the layer. A constant C is determined by the boundary condition. Starting with the appropriate boundary condition at the surface, the radiative transfer through a vertically inhomogeneous atmosphere is then simulated by dividing the atmosphere into a number of homogeneous layers and solving Eq. (3) successively for all layers. As a boundary condition at the surface, an emissivity of 1 is adopted in the WV channel for simplicity since the surface contribution to the outgoing radiance is negligibly small, i.e., the first term on the right-hand side of (1) cancels.

b. *Spectral resolution and atmospheric absorbers*

The WV channel of METEOSAT is sensitive to radiation between 5.7 and 7.1 μm, as is shown by the normalized filter function of the WV channel in Fig. 1. The filter function is calculated from the transmittance of the radiometer optics and the detector sensitivity at a temperature of 90 K at which the detector is operated. The curve is normalized to its maximum value of 0.52. Figure 1 also depicts the six spectral bands of the radiation scheme. The integration over the spectral bands with a weighting according to the filter function yields the radiances which correspond to the satellite measured count values.

Figure 2 shows an example of the radiance spectrum at the top of the atmosphere in the WV channel together with the six spectral bands of the radiation scheme. The solid line is the spectral radiance exiting a tropical standard atmosphere viewed in nadir direction. The dashed line is the spectral black-body radiance for the surface temperature of 300 K. The high resolution calculation was done with the radiation scheme described in Schmetz and Raschke (1981) and the computation of the optical depth makes use of Lowtran-5 data (Kneizys et al. 1980).

Neglecting the uniformly mixed absorbers in the Lowtran data-set causes noticeable changes in the outgoing radiance only at wavelengths outside the METEOSAT spectral response function. Therefore, in the radiation scheme for the WV channel, water vapor is the only absorber considered. The inclusion of CH_4, N_2O and CO_2 would change the result by less than 0.5% (Poc et al. 1980). In addition, Fischer et al. (1981) have shown that the O_2-induced absorption (Timofeev and Tonkov 1978) has a small influence on the calculated radiance in the WV channel. For a U.S. standard atmosphere, they have computed a decrease of 0.7°C in brightness temperature at nadir angle, which corresponds to a radiance change of less than 3%.

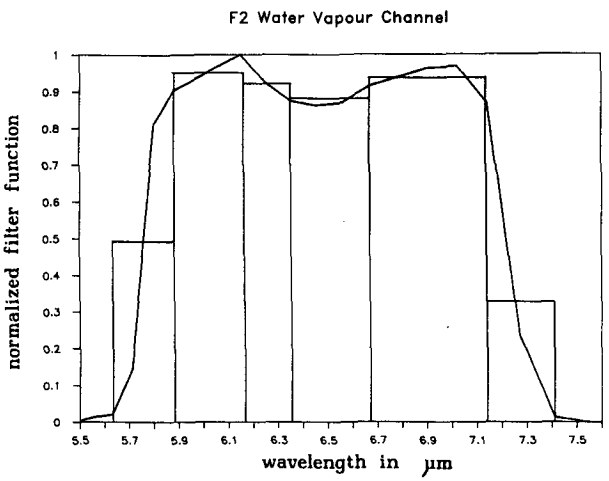

FIG. 1. Normalized filter function of the METEOSAT-2 water vapor channel and the six spectral bands of the radiation scheme used to compute theoretical radiances for the UTH retrieval.

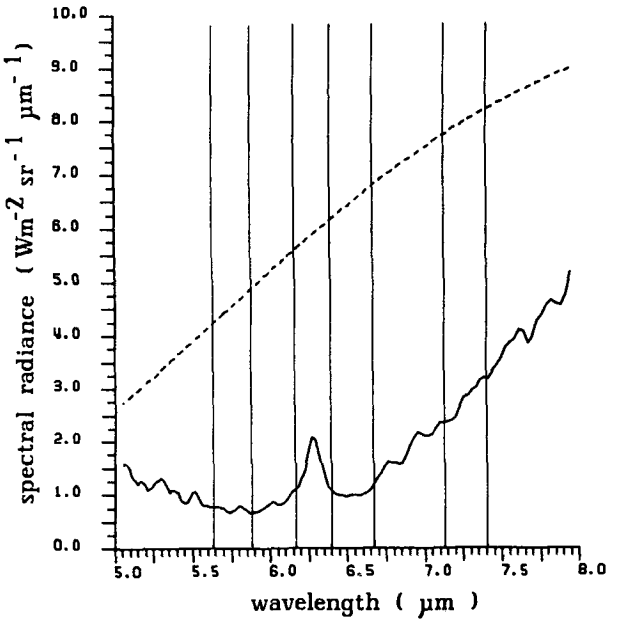

FIG. 2. Outgoing radiance at the top of a tropical standard atmosphere for nadir view ($\theta = 0°$). Dashed line indicates the surface Planck function. The vertical bars pertain to the spectral bands of the radiation scheme for the UTH retrieval.

The water vapor transmittance within each of the six spectral intervals of the radiation scheme is computed from an exponential-sum fit (Wiscombe and Evans, 1977):

$$\tau = \sum_{i=1}^{n} a_i \exp[-b_i f(\bar{c}, u)] \qquad (4)$$

with

$$f(\bar{c}, u) = u10^{\bar{c}},$$

where u is the equivalent absorber amount, $\bar{c}$ are spectral coefficients and $\sqrt{\tau}$ and $\bar{c}$ are based on Lowtran-5 (Kneizys et al. 1980). The a_i and b_i are the fit coefficients.

c. *Input data and vertical grid*

The forecast profiles of the temperature and humidity are routinely received from the ECMWF as ancillary data for the processing of the satellite image data. The 12 and 24 h forecasts are used for the 0000 and 1200 UTC UTH retrieval, respectively. The ECMWF data are available at standard levels for the temperature at 1000, 850, 700, 500, 400, 300, 250, 200, 150 and 100 hPa; for the mixing ratio from 1000 to 300 hPa; and for the geopotential height of the 1000 hPa level. For UTH retrieval, only forecast humidity values between 1000 and 600 hPa are used since the calculated radi-

ances are computed for constant relative humidities at pressure levels above 600 hPa (see section 3d). The ECMWF data are available on a 3° × 3° grid and they are interpolated to the segments for which the UTH product is estimated.

While the vertical grid provided by the ECMWF is considered to be sufficient for the specification of the atmospheric profiles, it is not necessarily adequate for the vertical integration of the radiative transfer equation. Therefore, additional levels are created by interpolation; the temperature is interpolated logarithmically in pressure; and the mixing ratios are interpolated so that the total precipitable water is kept constant.

The radiation scheme has been designed for a maximum of 20 levels, consisting of the surface pressure, the surface pressure minus 10 hPa, and levels at 50 hPa intervals from 950 to 100 hPa. Tests have shown that this resolution is not required for the operational application. A 14 level grid was found to be sufficient where the levels at 900, 750, 650, 550, 250 and 150 hPa are omitted. Thus, the relevant layer between 600 and 300 hPa is still resolved with five sublayers. Table 1 shows the differences in brightness temperature for four standard atmospheres and two zenith angles. The maximum difference is 0.5°C and the mean difference 0.2°C. Note also that the 14-level scheme is a reasonable compromise for radiative calculations in the IR window channel (Schmetz 1986). This 14-level scheme is, in the following, referred to as the operational radiation scheme.

d. UTH retrieval

Figures 3 and 4 illustrate what layers of the atmosphere contribute to the signal received at the satellite in the WV channel of METEOSAT-2. The normalized contribution functions are plotted for a tropical atmosphere and two zenith angles (Fig. 3), and for a tropical and a midlatitude winter atmosphere assuming a zenith angle of 62.7° (Fig. 4). This satellite zenith angle corresponds to the boundary of ESOCs operational processing at the 55° great circle arc. The outgoing radiance mainly originates from levels above about 4 km or about 600 hPa. For a tropical atmosphere and $\theta = 0°$, only about 10% of the outgoing radiance is emitted from layers beneath 600 hPa.

TABLE 1. Brightness temperatures (K) of outgoing WV radiance for four model atmospheres and two zenith angles (θ) as calculated with the 20-level radiation scheme and the operational 14-level version. Model atmospheres after McClatchey et al. (1972).

	$\theta = 0°$		$\theta = 62.7°$	
Model atmosphere	20 levels	14 levels	20 levels	14 levels
Midlatitude winter	242.1	242.0	237.2	237.2
Midlatitude summer	247.1	246.8	241.5	241.1
Tropical	248.5	248.2	242.8	242.3
Subarctic summer	243.8	243.8	239.0	239.1

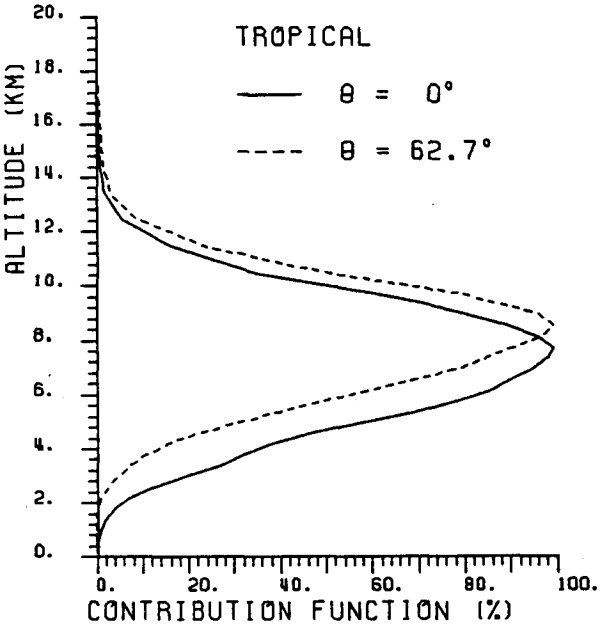

FIG. 3. Normalized contribution function for the METEOSAT-2 water vapor channel for a tropical standard atmosphere and satellite zenith angles of $\theta = 0°$ and $\theta = 62.7°$.

Figure 3 depicts how the peak of the contribution function moves upward with increasing zenith angle, and Fig. 4 indicates the difference between the moist tropical standard atmosphere (4.1 cm of precipitable water) and a dry (0.85 cm) midlatitude winter atmosphere.

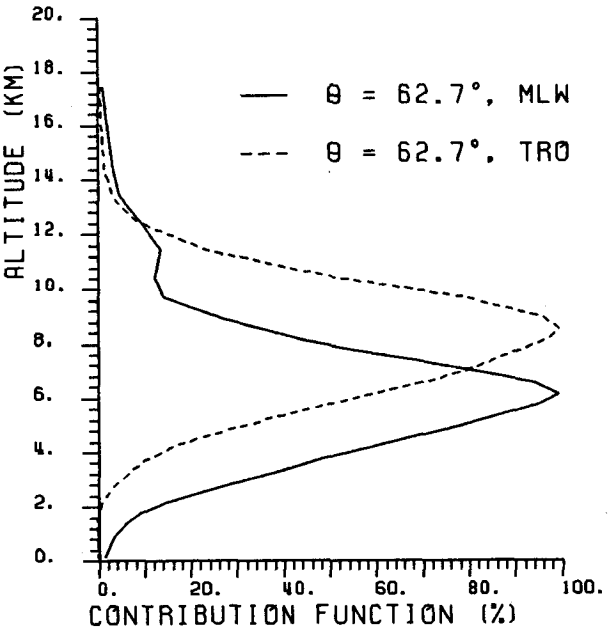

FIG. 4. As in Fig. 2 except for a tropical and a midlatitude winter atmosphere and a satellite zenith angle of 62.7°.

Figures 5 and 6 show the calculated outgoing WV and IR brightness temperatures for a tropical atmosphere as a function of the relative humidity which varied between 600 and 300 hPa for the two zenith angles of 0° and 62.7°. It is this type of information which is tabulated in the UTH tables to be used for the interpretation of the METEOSAT image data to estimate the UTH. The method for deriving the UTH is as follows:

(i) For each segment, radiative transfer calculations are performed for the WV and IR channel for relative humidities of 1%, 20%, 40%, 60%, 80%, and 100% at levels from 600 to 300 hPa (see Figs. 5 and 6). Above 300 hPa, the relative humidity decreases to 0% at 100 hPa. Radiation calculations encompass one set for clear sky and two for low-level cloud at 850 and 700 hPa, respectively.

(ii) The UTH tables provide the relative humidity as a function of the IR and WV counts. The count values are derived from the computed radiances of (i) with the corresponding calibration coefficients. The tables are ordered as a function of the IR counts. For a given range of IR counts, there is a set of humidities corresponding to WV counts.

(iii) The output of the segment processing is a description of everything identified, such as cloud within each segment. The UTH is not estimated for segments containing medium- or high-level cloud. For the remaining segments (land, sea, and low cloud) all clusters

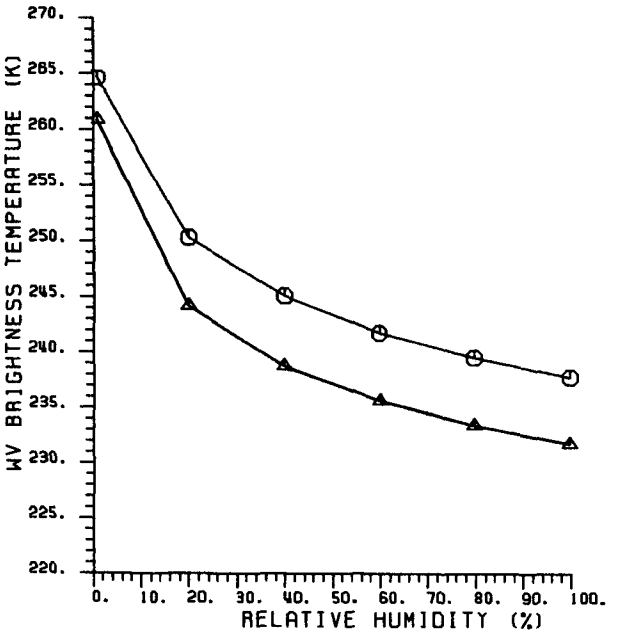

FIG. 5. Water vapor brightness temperature as a function of the relative humidity of the upper troposphere (600 to 300 hPa) for a tropical standard atmosphere and zenith angles of 0° (octagons) and 62.7° (triangles). The filter function of METEOSAT-2 is assumed.

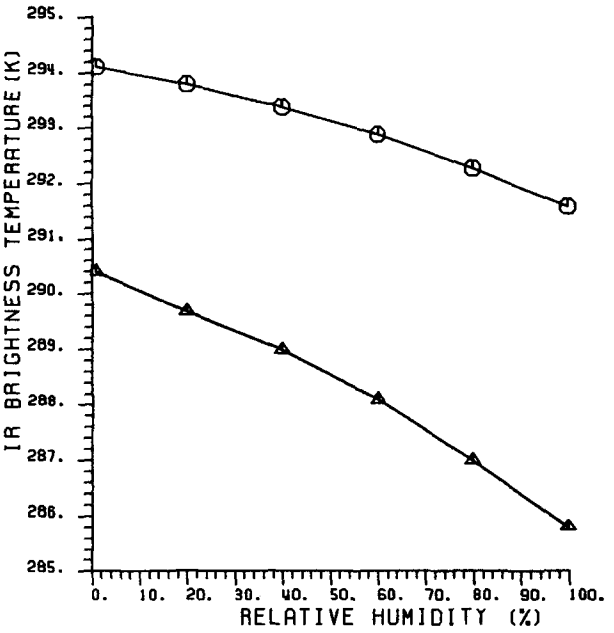

FIG. 6. Infrared brightness temperature as a function of the relative humidity of the upper troposphere (600 to 300 hPa) for a tropical standard atmosphere and zenith angles of 0° (octagons) and 62.7° (triangles). The filter function of METEOSAT-2 IR-1 is assumed.

are combined into a mean radiance for the IR and WV channels. These mean radiances are then used to estimate the UTH product.

(iv) As the first step in calculating the desired humidity, the measured IR count is interpolated in the precomputed table. The second interpolation finds the best match for the measured WV count within the table relationship between WV count and relative humidity. The UTH tables contain the IR as a variable, but the WV radiance actually provides the final estimate of the UTH in a segment. The purpose of the IR dependence is to avoid ambiguities related to the occurrence of low-level cloud. For example, a low-level cloud in a segment with a given UTH could yield the same WV radiance as the clear sky segment with a somewhat higher UTH. However, the IR dependence has only a marginal impact on the retrieval, only when the upper troposphere contains little water and thus allows the lower troposphere to contribute to the WV signal at the satellite. An example of a UTH table is given in Table 2.

(v) The UTH is not derived where the measured WV count fails to fall within the precomputed interval set by the UTH table. This applies to 1%–2% of the data.

4. Comparison of the WV radiation scheme with other models

To validate the atmospheric radiation scheme for the WV channel we have compared contribution func-

TABLE 2. Example of a UTH table. Atmospheric profile is characteristic of a tropical atmosphere, except that the relative humidity from 600 to 300 hPa has been changed to fixed values indicated in the table. Zenith angle is 0°.

Type	Relative humidity (%) between 600 and 300 hPa					
	1	20	40	60	80	100
Water vapour counts	58	39	33	30	28	26
IR window counts	139	138	137	136	135	134

tions as calculated with a radiation scheme using the transmittance parameterization described in section 3b with the results presented by Fischer et al. (1981). The Fischer radiation model is based on a polynomial representation of the transmittances for wavenumber intervals of 25^{-1} cm. The polynomials were fitted to line-by-line results. Our calculations make use of the emissivity method (e.g., Stephens 1984), since the analytical scheme described above does not provide contribution functions. Both methods are in agreement for the outgoing radiance. Note that the comparison is based on the filter function for METEOSAT-1 (Morgan 1978), which is somewhat different from that of METEOSAT-2 (see Fig. 1).

The contribution function which is compared in Table 3 is defined by

$$\chi = \int_{\lambda_1}^{\lambda_2} \phi(\lambda) B(T) \frac{\partial \tau}{\partial p} d\lambda \qquad (5)$$

where λ_1 and λ_2 indicate the cutoff wavelengths of the filter function ϕ of the radiometer.

Results of the comparison with Fischer et al. (1981) can be summarized as follows: Generally speaking, there is good agreement between our scheme and the Fischer radiation model. The maximum difference for the peak of the contribution function is 300 m in case of the tropical standard atmosphere. The half-width intervals also agree within 200 m.

TABLE 3. Maximum and half-width range of the contribution function for the METEOSAT-1 IR-2 channel, for different standard atmospheres and different zenith angles. Calculations with the ESOC scheme are compared with the results of Fischer et al. (1981) which are given in parentheses. Standard atmospheres are those given by McClatchey et al. (1972).

Model atmosphere	Zenith angle (deg)	Maximum of contribution function (km)	Half-width range (km)
Tropical	0.0	7.3 (7.0)	4.5–10.2 (4.1–9.7)
	62.7	8.4 (8.2)	5.6–10.5 (5.2–10.1)
Midlatitude winter	0.0	5.5 (5.5)	2.3–7.4 (2.2–7.4)
	62.7	6.1 (6.0)	3.5–7.8 (3.5–7.7)

Table 4 shows a comparison of the operational radiation scheme with results of detailed study of the WV channel by Poc et al. (1980). They have calculated the outgoing radiance for model atmospheres assuming the METEOSAT-1 filter function. The model atmospheres are modifications of the midlatitude standard atmosphere and the zenith angle $\theta = 50°$. The ESOC scheme yields radiances which are slightly—and consistently—lower than those of Poc et al., but the relative changes of radiances with modification of the model atmosphere are very similar. Small systematic differences are easily explained by slightly different discretization of the filter function of the radiometer (see Fig. 1).

As a final comparison, Table 5 presents results of radiance calculations using a measured atmospheric profile after Eyre (1980). This profile was measured by instruments on a research aircraft over the eastern Atlantic on 29 November 1978. The experiment was then undertaken to provide an absolute calibration of the METEOSAT-1 WV channel. From the measured profile of temperature and humidity, Eyre calculated the brightness temperature at the top of the atmosphere for the satellite zenith angle of 38.8° using the LOWTRAN 3B model, a Goody random band model, and a Malkmus random band model respectively. His results are repeated in Table 5 for comparison with the brightness temperature obtained with the ESOC radiation scheme.

Based on the fair agreement with the other studies, the conclusion is made that the ESOC scheme is suited for the computation of radiances to set up the UTH interpretation tables.

5. Calibration of the 6.3 μm channel

In remote sensing, a proper calibration of an instrument is a prerequisite for the quantitative use of its data. Thus, the METEOSAT 6.3 μm water vapor (WV)

TABLE 4. Comparison of radiances for different model atmospheres between the model of Poc et al. (1980) and the ESOC scheme. Results are based on the filter function of METEOSAT-1 IR-2. Zenith angle is $\theta = 50°$.

Model atmosphere	Radiance (W m^{-2} sr^{-1})	
	Poc et al.	ESOC scheme
Midlatitude summer	0.79	0.77
+5% relative humidity between 1000 and 200 hPa	0.77	0.74
−5% relative humidity between 1000 and 200 hPa	0.83	0.81
50% relative humidity between 1000 and 200 hPa	0.71	0.68
70% relative humidity between 1000 and 200 hPa	0.65	0.63

TABLE 5. Calculated brightness temperature (BT) for three different radiation schemes after Eyre (1980) for a measured atmospheric profile and the result from the present ESOC radiation scheme.

Radiation model	Lowtran 3b	Goody model	Malkmus model	ESOC scheme
BT (°C)	−21.52	−21.96	−21.50	−21.3

channel must be calibrated to allow its use in quantitative applications. Unfortunately, no calibration of the WV channel is performed onboard the satellite, and no other direct measurements at 6.3 μm are available. Instead, some measurements that can be related to the radiances at 6.3 μm must be used. For example, observed temperature and humidity profiles can be converted into radiances (hereafter called pseudoradiances) using the radiative transfer model. The accuracy of the resulting pseudoradiances is probably compromised by the fact that mid- and upper-tropospheric humidity measurements tend to have fairly large errors. The temperature and humidity data originate from the radiosonde network.

The UTH plays a secondary role in the calibration process, since the quality of the calibration coefficient is monitored by following the behavior of the bias between the UTH and in situ humidities. A new calibration coefficient, calculated for each run, is not introduced automatically. If the bias remains within certain limits, no change of the calibration is made. The calibration coefficient is updated only if the bias becomes larger than 5% for a number of consecutive runs. This is a precaution taken to avoid too frequent and unnecessary changes of the calibration coefficient, caused by random errors of the observed humidities. The calculation of the calibration coefficient is described below.

a. Data

Two types of data are needed for the calibration: observed WV counts averaged over a segment, and radiosonde data. Only WV counts originating from segments without medium or high clouds are taken into account. There are about 2000 segments with valid UTH data for the METEOSAT processing area for each run.

Radiosonde reports are limited, since only 100–150 stations report regularly in the area seen by METEOSAT. In addition, the radiosonde stations are not geographically evenly distributed, since about 60% are located between 20° and 55°N. The equatorial belt is normally represented by about 20 stations only, and the Southern Hemisphere is typically covered by 25 sondes only. All radiosonde stations that are located in the segments with valid UTH values are used for the comparison. As a result, typically about 25 collocated radiosondes with valid UTH values are found.

b. Method

The temperature and humidity profiles from the radiosondes are converted into pseudoradiances R corresponding to the values obtained from the WV channel. The conversion is done using the radiative transfer model as described in section 3. A pseudocount is also determined using the valid calibration equation and the pseudoradiance. To filter out gross observational errors, only 6 μm pseudocounts, deviating less than eight counts from the observed, are considered. (The radiometric resolution of the WV-channel is 64.) Due to this quality control, about 15% of the collocated points are disregarded. An average of the accepted pseudoradiances is determined, and the slope (A6) of the calibration equation is calculated by relating the average of the pseudoradiances R and observed counts C in the following equation:

$$R = \mathrm{A6}(C - SC) \tag{6}$$

where R is the pseudo radiance, C the mean observed WV count, and SC the (constant) space count.

The method used is not based on the least-squares fit, but is simply a straight line through the space count and the mean value.

c. Monitoring

To monitor the quality of the calibration, the UTH is compared with a weighted mean humidity based on radiosonde data. The weights are obtained from an average contribution function counted for a standard midlatitude summer atmosphere. The radiosonde humidity originates from four levels (600, 500, 400 and 300 hPa). These four levels correspond to the layer characterized by the UTH. Only the stations with all the four levels are considered. In the determination of the radiosonde humidity, the seasonal and geographical variations of the contribution function profile are not yet taken into account. This may limit the utility of the radiosonde humidity as, in principal, the average humidity from radiosondes must be calculated with the correct contribution function. Further study is required to quantify the error.

An example of the monitoring of the quality of the calibration coefficient is shown in Table 6. It can be

TABLE 6. Comparison of the UTH with the radiosonde humidity (R/S humidity) to monitor the calibration of the 6.3 μm channel for 20 July 1987 (2300 UTC). Valid 6 μm calibration equation was $R = 0.0294(C - 3)$, and the suggested 6 μm calibration equation was $R = 0.0305(C - 3)$. 22 collocated points were found, but only 21 collocated points were considered after the quality control. A6 is in W m^{-2} Sr^{-1} ct^{-1} (6 bit counts).

Variable	Mean (%)	Standard deviation (%)
UTH − R/S humidity	6.0	9.6
UTH	32.0	9.6
R/S humidity	26.0	10.9

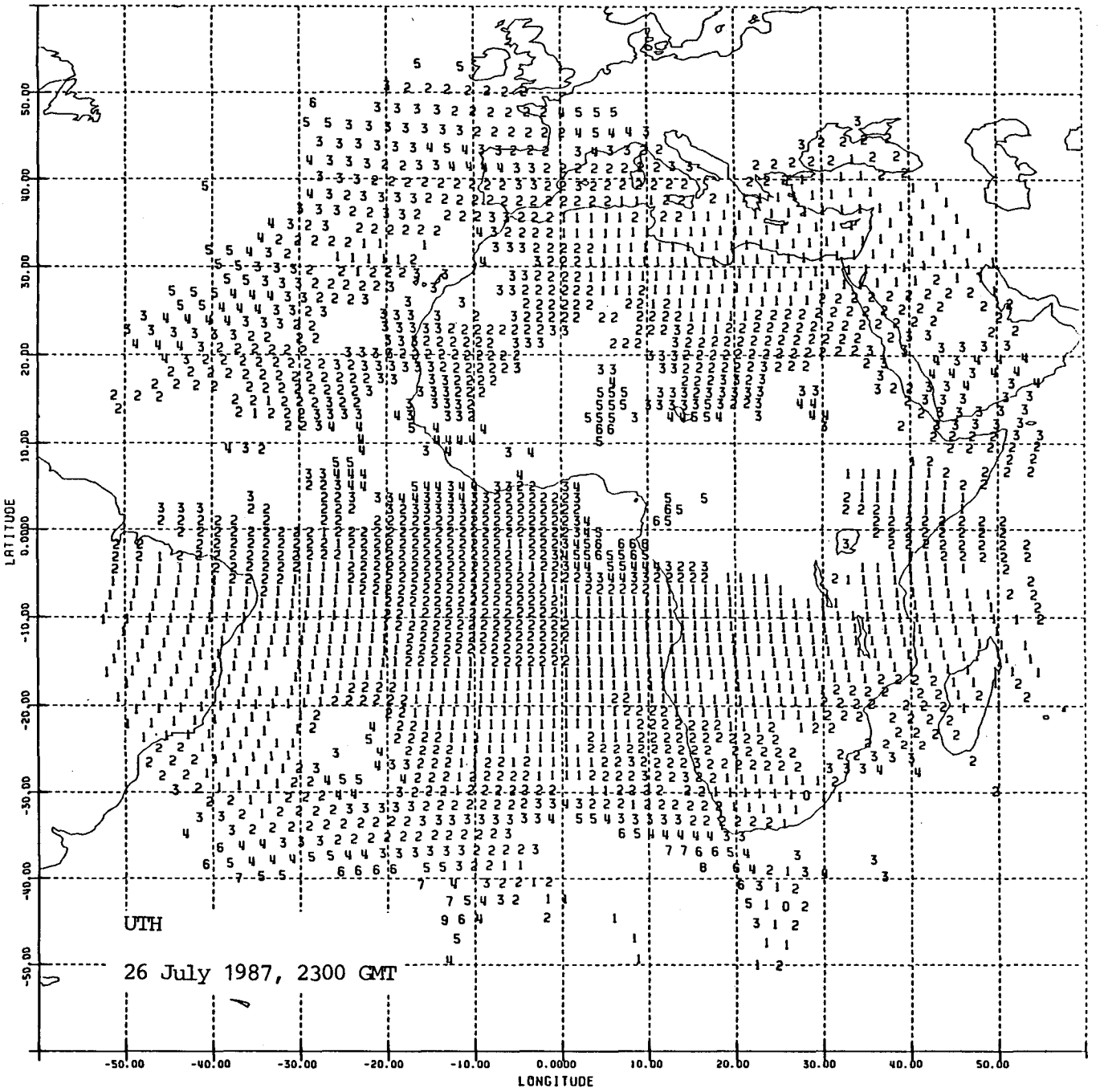

FIG. 7. (a) Typical coverage of the UTH product, 26 July 1987 (values are in 10%).
(b) Typical locations for radiosondes 26 July 1987 (values are in %).

seen that the bias between radiosonde and satellite humidities was larger than 5%. Therefore, the newly calculated coefficient was introduced.

Figures 7a and b illustrate typical coverages of the UTH-values and weighted mean radiosonde humidities, respectively, over the METEOSAT processing area.

6. Error estimation

The UTH derivation is based on different data, all having a certain error characteristic which, in turn, affect the quality of the UTH product. In this section we try to quantify the accuracy of the UTH.

The precision of the satellite measurements is known

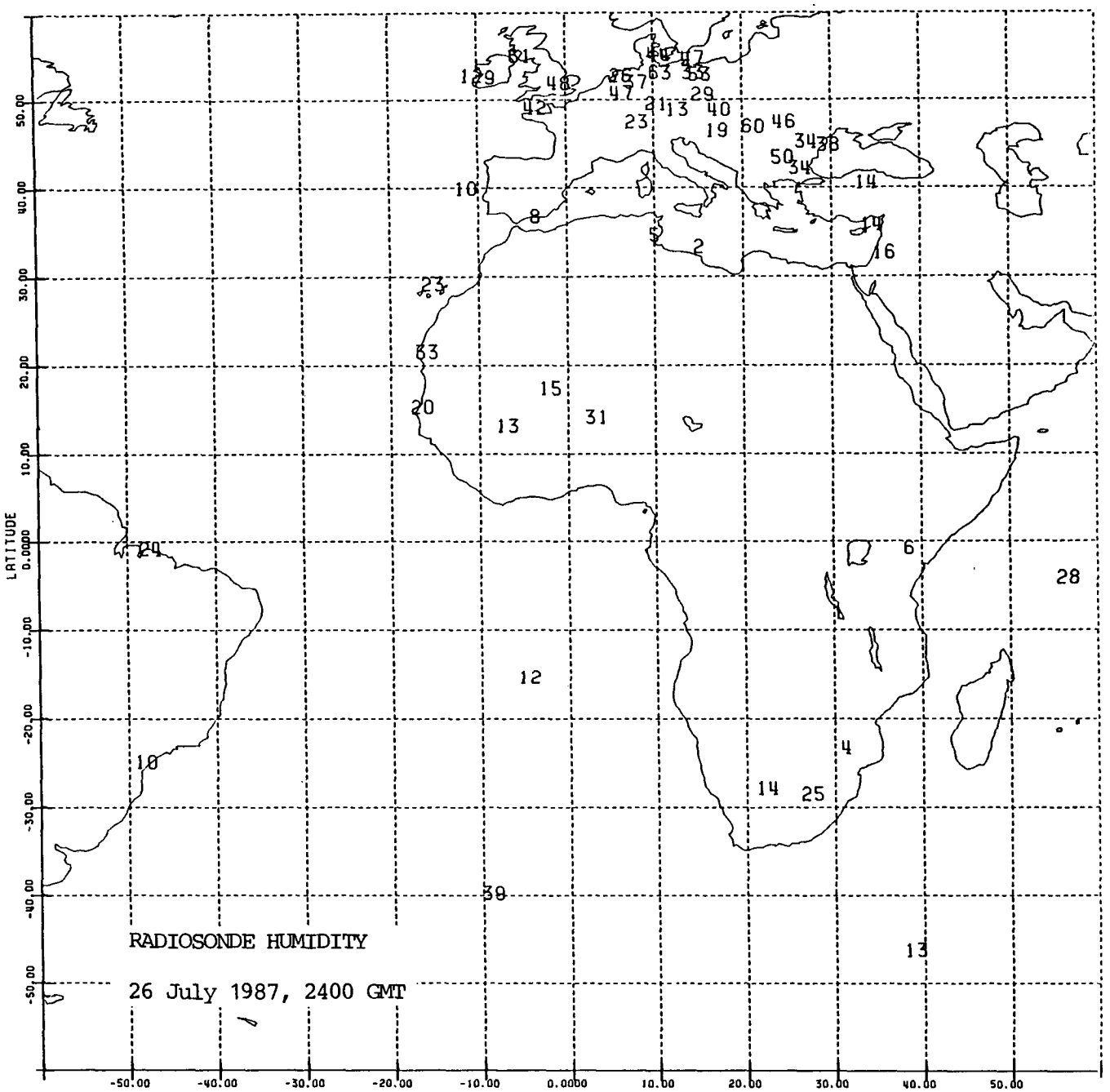

FIG. 7. (*Continued*)

from the prelaunch tests for the WV channel. For a scene temperature of 260 K, the $NE\Delta T$ is about 0.5°C. The noise should be negligible since, in practice, the actual mean radiances are for a segment of 1024 pixels. The absolute accuracy is ultimately determined by the vicarious calibration as described in section 5. Hence, it depends on the accuracy of the radiosonde measurements, and whether the radiosonde is representative for the segment area, and, of course, on the radiation scheme. The latter has been checked to some extent in section 4 by comparison with other model results.

The UTH retrieval is affected by errors in the temperature forecast profile, the humidity profile between the surface and 600 hPa, and the assumed humidity profile above the 300 hPa level. Also, the assumption of a constant relative humidity between 600 and 300 hPa is not realistic.

A simple sensitivity test which shifts the forecast profiles by certain increments helps to reveal the error characteristics of the UTH retrieval. Table 7 shows the results of such a test, assuming a tropical standard atmosphere and a spacecraft zenith angle of 0°. The first row in Table 7 gives the brightness temperatures for the original profile with the relative humidity modified between 600 and 300 hPa as in section 3d. The test produces shifts of the temperature profile by +1° and +2°C, respectively, and shifts of the relative humidity by +20% (absolute) between 600 hPa and the surface, and 300 and 100 hPa, respectively.

The errors in the temperature forecast have a relatively small impact. This situation occurs because of the increase of absolute humidity with temperature, which lifts the contribution function to higher and colder levels and thus counteracts the increase in brightness temperature caused by the temperature shift.

The humidity between the surface and the 600 hPa level is an uncritical parameter which is not surprising when we consider the dependence of the contribution function on altitude. By contrast, the humidity profile above the UTH layer from 600 to 300 hPa is quite important. Remember, we simply let the relative humidity decrease from the 300 hPa value to 0% at 100 hPa, which seems to be a reasonable assumption in line with the structure of standard profiles. The last row in Table 7 indicates that a 20% shift of the humidity causes a change in brightness temperature which is the equivalent of roughly a 10% change in the UTH product.

In summary, we estimate an error of the UTH of the order of 10 to 15%. For low relative humidities the uncertainty in the structure of the humidity profile above 300 hPa and also within the UTH layer are the major error sources. The coarse 6-bit digitization becomes equally important at high humidities, where a change of 1°C in brightness temperature (which is about 1 count) corresponds to relative humidity changes of about 10%. In practice, the latter may not be so important; at high humidities, the occurrence of cloud is more likely, and the present retrieval is confined to segments without medium- or high-level cloud.

TABLE 7. Brightness temperature (K) of the outgoing radiance in a standard tropical atmosphere for a spacecraft zenith angle of 0°. Columns pertain to the different humidity classes used to compute the UTH tables, and rows give results for various perturbations of the temperature and humidity profile.

	Relative humidity between 300 and 600 hPa (%)					
Profile	1	20	40	60	80	100
"original"	264.6	250.3	245.1	241.8	239.6	237.8
$T = +1$°C	265.3	250.6	245.3	242.1	239.7	238.0
$T = +2$°C	266.0	250.8	245.5	242.3	239.9	238.2
Humidity shift 20% below 600 hPa	264.4	250.2	245.0	241.8	239.5	237.8
Humidity shift 20% above 300 hPa	259.9	248.5	243.7	240.9	238.7	237.1

The difference between the UTH and radiosonde humidities is depicted in Fig. 8, where a scatter plot for a period of 25 days including 1035 comparisons is shown. Mean values are 28.8% for the UTH and 27.7% for the radiosonde relative humidity. The rms error is 10.2%. The standard deviation for the radiosondes (14.6%) is slightly higher than that for the UTH (12.9%) which is consistent with the fact that radiosonde measurements also capture variability at smaller scales than the UTH.

7. Summary and conclusion

This study has described a method to estimate the mean upper tropospheric relative humidity (UTH) from the radiance measurements in the 6.3 μm water vapor channel of the geostationary satellite METEOSAT. The radiance measurements are converted into relative humidities via tables which are computed with a radiative transfer scheme. The radiation scheme uses the 12 and 24 h forecast profiles for temperature and for the humidity up to 600 hpa from the ECMWF as model input data. The radiation scheme resolves the 6.3 μm channel with six spectral intervals. Transmittances are calculated from an exponential sum fit. Comparison of the scheme with other models shows good agreement.

The quantitative evaluation of the satellite data requires calibrated data. The WV channel is operationally calibrated with the aid of the radiative transfer scheme using radiosonde profile data and the colocated WV counts as measured by the satellite. The operational calibration coefficient is only changed if the monitoring procedure suggests a UTH bias of about 5% (for details see chapter 5). While this way of calibration seems sufficient for the UTH retrieval, the arbitrary character of changing the coefficient requires a revision in the near future.

A comparison of 1035 UTH values with collocated radiosondes yields a mean difference of 1.1% and an rms error of 10.2%.

At present, the UTH is estimated twice daily at 0000 and 1200 UTC and disseminated as SATOB code via the Global Telecommunication System (GTS). The product is intended to be used in the data analysis for the numerical weather prediction as additional information to the routinely used SATEM moisture data from polar-orbiting satellites. The impact of the additional data needs to be assessed in a future study. One could expect a beneficial impact on numerical forecast models, as Heckley (1985) has pointed out the importance of having the energy balance of the atmosphere correct at the start of a forecast. Here, the UTH observations could provide a better initial estimation of the upper tropospheric longwave radiative cooling and shortwave heating, which, in turn, could lead to a better description of the radiative destabilization of the atmosphere.

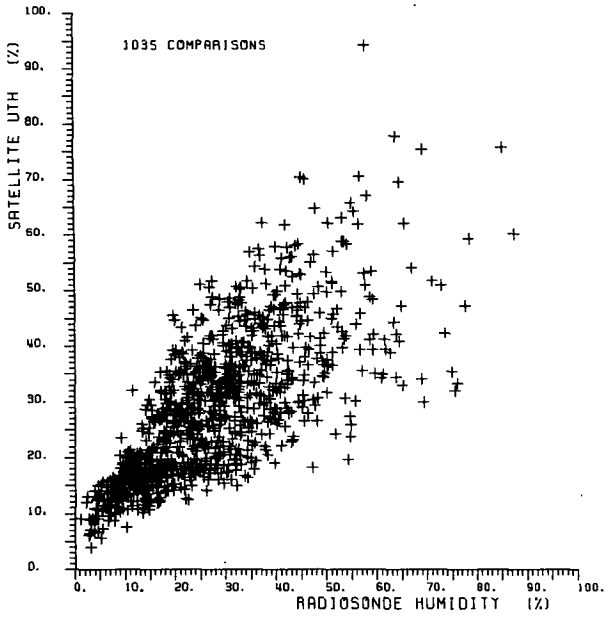

FIG. 8. A scatter plot of the UTH versus radiosonde humidity determined with an average contribution function. Mean values for the UTH and the radiosondes are 28.8% and 27.7%, respectively. The rms error is 10.2%.

A systematic validation of the UTH will be the subject of forthcoming work. It will include a longer-term comparison of UTH and radiosonde humidity data.

Acknowledgments. We wish to thank Mr. Quanhua Liu for carrying out the computations for the error estimation. Thanks are also due to Mr. Brian Mason for carefully reading the manuscript and helpful suggestions. The detailed comments of the reviewers were appreciated.

REFERENCES

de Waard, J., M. Fea and A. Robson, 1984: The METEOSAT Exploitation Project: Operational use of a remote sensing system. *Earth-Orient. Applic. Space Technol.*, **4**, 227–237.

Eyre, J. R., 1980: Calibration and some exploratory uses of METEOSAT water vapour channel imagery. *Proc. Second METEOSAT Scientific User Meeting*, London.

Fischer, H., N. Eigenwillig and H. Müller, 1981: Information content of METEOSAT and Nimbus/THIR water vapor channel data: Altitude association of observed phenomena. *J. Appl. Meteor.*, **20**, 1344–1352.

Hayden, C. M., W. L. Smith and H. M. Woolf, 1981: Determination of moisture from NOAA polar orbiting satellite sounding radiances. *J. Appl. Meteor.* **20**, 450–466.

Heckley, W. A., 1985: Systematic errors of the ECMWF operational forecasting model in the tropical regions. *Quart. J. Roy. Meteor. Soc.*, **111**, 709–738.

Illari, L., 1987: The quality of satellite PWC data and their impact on the ECMWF humidity analysis. Accepted by *Tellus* A.

Kneizys, F. X., E. P. Shettle, W. O. Gallery, J. H Chetwynd, L. W. Abreu, J. Selby, R. W. Fenn and R. A. McClatchey, 1980: Atmospheric transmittance/radiance, Computercode Lowtran-5, AFGL-TR-0067, Air Force Geophysics Laboratory, Bedford, MA.

Liou, K. N., 1980: *An Introduction to Atmospheric Radiation.* Academic Press, 392 pp.

McClatchey, R. A., R. W. Fenn, J. Selby, F. E. Volz and J. J. Garing, 1972: Optical properties of the atmosphere. AFCRL-72-0497, 108 pp.

Möller, F., 1961: Atmospheric water vapor measurements at 6–7 microns from a satellite. *Planet. Space Sci.*, **5**, 202–206.

Morgan, J., 1978: Introduction to the METEOSAT system. MDMD-Met Issue 1, European Space Operations Centre, Darmstadt, FRG.

Poc, M., M. Rolleau, N. A. Scott and A. Chedin, 1980: Quantitative studies of METEOSAT water-vapor channel data. *J. Appl. Meteor.*, **19**, 868–876.

Raschke, E., and W. R. Bandeen, 1967: A quasi-global analysis of tropospheric water vapor content from TIROS-IV radiation data. *J. Appl. Meteor.*, **6**, 468–481.

Schmetz, J., 1986: An atmospheric-correction scheme for operational application to METEOSAT infrared measurements. *ESA Journal*, **10**, 145–159.

——, and E. Raschke, 1981: An approximate computation of infrared radiative fluxes in a cloudy atmosphere. *Pure Appl. Geophys.*, **119**, 248–258.

Stephens, G. L., 1984: The parameterization of radiation for numerical weather prediction and climate models. *Mon. Wea. Rev.*, **112**, 826–867.

Timofeyev, Y., and M. V. Tonkov, 1978: Effect of the induced oxygen absorption band on the transformation of radiation in the 6 um region in the earth's atmosphere. *Izv. Atmos. Ocean. Phys.*, **14**, 437–441.

Wiscombe, W., and J. Evans, 1977: Exponential-sum fitting of radiative transmission functions. *J. Comput. Phys.*, **24**, 416–444.